From Simple Liquid to Polymer Melt. Glassy and Polymer Dynamics Studied by Fast Field Cycling NMR Relaxometry: Low and High Molecular Weight Limit

S. Kariyo,[†] A. Brodin,[§] C. Gainaru,[§] A. Herrmann,[§] H. Schick,[§] V. N. Novikov,[‡] and E. A. Rössler*[,§]

Faculty of Science and Technology, Yala Islamic University, 135/8 M.3, T. Khaotoom A.Yarang, Pattani 94160, Thailand; IA&E, Russian Academy of Sciences, Novosibirsk 630090, Russia; and Experimentalphysik II, Universität Bayreuth, 95440 Bayreuth, Germany

Received December 12, 2007; Revised Manuscript Received April 23, 2008

ABSTRACT: Fast field cycling (FFC) NMR is applied to study the dispersion of the ^{1}H spin−lattice relaxation in the low molecular weight glass-formers *o*-terphenyl, tristyrene, and oligomeric polybutadiene (PB, with M/gmol^{-1} = 355 and 466) over a broad temperature range (203−401 K). Differing from previous FFC NMR works, we analyze the relaxation data in the susceptibility form $\omega/T_1(\omega)$, and applying frequency−temperature superposition, master spectra are obtained covering up to 8 decades in frequency. In all cases solely the glassy dynamics (α-process) determines the relaxation behavior, and the Rouse unit is estimated to $M_R \cong 500$ g/mol. The time constant $\tau_\alpha(T)$ in the range $10^{-11}-10^{-6}$ s is extracted, which agrees well with those measured at the same time by dielectric spectroscopy. For the high molecular weight PB (M/gmol^{-1} = 56 500, 87 000, 314 000, and 817 000) pronounced polymer effects are observed at low frequencies ($\omega\tau_\alpha \ll 1$) which are isolated from the total spectrum by subtracting the "glass spectrum" as obtained from low molecular PB. We argue that unless the underlying α-relaxation is properly accounted for, the apparent power law spectrum does not reflect the actual polymer dynamics.

I. Introduction

At temperatures around and below the melting point, the dynamics of (supercooled) molecular (monomeric) liquids is governed by the glass transition phenomenon with its characteristic two-step correlation functions that exhibit a stretched long-time part due to the structural relaxation or α-process.[1–3] Connecting monomers into linear chains leads to further polymer-specific relaxation processes that are slow with respect to the α-relaxation time scale τ_α, the latter in the case of polymers being attributed to the local segmental dynamics of the chains. Depending on the molecular weight M, the collective dynamics due to connectivity of the chains are described either by the Rouse model below the entanglement threshold M_e or by the reptation model ($M > M_e$), where M_e denotes the average molecular weight between entanglements.[4–6] Starting from a monomer and increasing the chain length, one expects first the Rouse dynamics to set in at a certain characteristic M_R, followed thereafter by the reptation dynamics at $M < M_e$. Whereas many studies addressed the crossover from Rouse to reptation dynamics, significantly less attention is given to the crossover from a monomeric liquid dynamics to the Rouse regime.[7–11] The long-standing question "when is a polymer a polymer?"[12] has been reassessed in, e.g., a recent work by Ding et al.,[10] yet a satisfactory answer is still missing.

Recently, we have reported preliminary results of a fast field cycling (FFC) NMR study of a series of 1,4-polybutadienes (PB), covering a broad range of molecular weights.[11] FFC NMR determines frequency dispersion of the spin−lattice relaxation time $T_1(\omega)$ that, in the present context, reflects the spectrum of reorientational dynamics of a polymer segment.[13–17] We found that the relaxation effects due to polymer dynamics in PB set in at $M \cong 500$ and thereafter saturate at $M > \cong 4000$ due to entanglement. The characteristic Rouse unit size is therefore $M_R \cong 500$, which compares well with results from other experiments.[18–21] We also found that the relative degree of orientational correlation, relaxed by the polymer dynamics alone and related to the so-called dynamic order parameter,[22–26] is significantly larger than expected.[15,16] These findings agree with the results of a double-quantum NMR study on PB[24,25] that also concluded a quite high dynamic order parameter. We thus argued that a polymer melt might possess a significant degree of orientational order, perhaps higher than usually assumed.

In the present contribution, we introduce further FFC NMR results and analyses of a series of 1,4-polybutadienes covering molecular weights in the range $355 < M_w < 817\,000$, aiming to achieve a better understanding of the relaxation in linear polymers in relation to polymer and glassy dynamics. We shall argue that in order to quantitatively analyze FFC NMR spectra, e.g., in terms of the Rouse theory, the contribution due to the polymer dynamics has to be separated from the much stronger and ever-present spectrum of local segmental motion, the latter analogous to the α-relaxation of simple liquids and therefore dubbed "glassy dynamics" in the following. As a reference for a pure glassy dynamics, we consider relaxation data of two molecular liquids, *o*-terphenyl and tristyrene. Differing from previous FFC NMR analyses,[13,15,16] we present the relaxation data $T_1(\omega)$ in the form $\omega/T_1(\omega)$,[11] which to a good approximation is proportional to the susceptibility related to segmental reorientation correlation function of second rank. FFC NMR data in the susceptibility representation can be directly compared with the susceptibility data of other experiments.

In addition to FFC NMR, all the samples are characterized by dielectric spectroscopy.[11,27] PB is a "type B" polymer,[27–29] meaning that there is no contribution from the polymer dynamics in the dielectric spectrum, and therefore the latter exclusively reflects the segmental motion. This enables us to accurately determine the segmental relaxation time constant τ_s for comparisons with the FFC NMR data. In this way, we identify the segmental time constant τ_s with the structural relaxation time τ_α. Discussing the meaning of the relatively high dynamic order parameter obtained from our analysis, we will argue that this

* Corresponding author.
[†] Yala Islamic University.
[‡] Russian Academy of Sciences.
[§] Universität Bayreuth.

10.1021/ma702771s CCC: $40.75
Published on Web 06/26/2008

does not necessarily imply an equally high static orientational order in the melt. Overall, we hope to offer a new view as to when a molecule becomes a polymer and to demonstrate that FFC NMR is a potent tool for investigating these effects.

The present contribution is the first part of a series of two papers on FFC NMR investigations of high and low molecular weight systems. In section II, we introduce the necessary theoretical background of FFC NMR and present in section III the experimental data of PB in the limiting cases of low and high molecular weights. In section IV, we will present data of a series of PB homologues with systematically varied molecular weight that display the crossover from simple liquid to polymer melt. The data will be analyzed in the frame of Rouse theory.

II. Theoretical Background

A. Spin−Lattice Relaxation. Fast field cycling (FFC) NMR is a well-established method for studying molecular dynamics in condensed matter, based on determining the frequency dispersion of spin−lattice relaxation time $T_1(\omega)$.[13–17] The method is particularly suited to study slow dynamics in polymer melts.[15] In the case of the ^{1}H nucleus, the decay of magnetization expressed by T_1 is due to fluctuations of the dipolar interactions of proton spins. The interaction Hamiltonian then involves a sum over all pairs of spins i, j in the sample. The interaction term of a particular pair of spins ij, separated by $\mathbf{r}_{ij}$, depends on the polar ϑ and azimuthal φ angles with respect to the magnetic field as well as on the distance r_{ij}. The sum can be separated into intra- and intermolecular contributions that, assuming their statistical independence, contribute additively to the relaxation rate:[15,16]

$$1/T_1 = 1/T_1^{\text{intra}} + 1/T_1^{\text{inter}} \tag{1}$$

However, because of the short-range nature of dipole−dipole interaction, one expects that the main contribution to the interaction sum comes from the nearest proton pairs belonging to the same molecular units and that intermolecular terms are relatively unimportant. Numerous works attempted to separate orientational and translational contributions in proton NMR.[30–32] In the case of polymers, direct comparisons of ^{1}H and ^{2}H NMR relaxation data, the latter only sensitive to molecular reorientation dynamics, indicate that indeed intermolecular translation dynamics only shows up at very low frequencies in ^{1}H NMR.[15,16,33] We thus assume, in the present context, that distinct intermolecular contributions are negligible, so that our NMR data mostly reflect segmental reorientation dynamics, so that $T_1 \approx T_1^{\text{intra}}$.

Orientational dynamics enters the calculation of relaxation rate $1/T_1$ through the correlation functions F_2^m of the second rank spherical harmonics $Y_{2,m}(\vartheta,\varphi)$[13–15,34]

$$F_2^m(t) = \langle Y_{2,m}(\vartheta_0,\phi_0) Y_{2,-m}(\vartheta_t,\phi_t)\rangle / \langle |Y_{2,m}(\vartheta_0,\phi_0)|^2 \rangle \tag{2}$$

where the indices 0 and t refer to the initial and final times, respectively. Orientational average for a macroscopically isotropic system yields an m-independent expression for the orientational correlation function, expressed through the second-rank Legendre polynomial $P_2(\cos\vartheta) = {}^1/_2(3\cos^2\vartheta - 1)$[16,35]

$$F_2(t) = \langle P_2(\cos\vartheta_0)\, P_2(\cos\vartheta_t)\rangle / \langle |P_2(\cos\vartheta_0)|^2 \rangle = \langle P_2(\cos(\vartheta_t - \vartheta_0))\rangle \tag{3}$$

with the corresponding spectral density

$$J(\omega) = \mathrm{Re}\int_0^\infty F_2(t) e^{-i\omega t}\, dt \tag{4}$$

The correlation time τ of the orientational fluctuations is given by the integral over the correlation function

$$\tau = \int_0^\infty F_2(t)\, dt = J(0) \tag{5}$$

The ^{1}H spin−lattice relaxation rate $1/T_1$ is then related to the spectral density $J(\omega)$ through the well-known Bloembergen, Purcell, and Pound equation[36]

$$1/T_1(\omega) = C[J(\omega) + 4J(2\omega)] \tag{6}$$

where $\omega = \gamma B_0$ is the Larmor frequency depending on the gyromagnetic ratio γ and magnetic field B_0, whereas C is a coupling constant, which depends on the nuclear separation r_{ij} of the spin pairs.[34] In a FFC NMR experiment, the field B_0 and thus the Larmor frequency ω are varied, so that the dispersion of relaxation rate $1/T_1(\omega)$ provides access to the spectral density $J(\omega)$.

The spectral density of thermal equilibrium fluctuations of a property, such as $J(\omega)$ that describes molecular orientational fluctuations, is related by the fluctuation−dissipation theorem to the linear response of that property to a weak external perturbation, i.e., to a response (susceptibility) function. Specifically, the loss (imaginary) part of the susceptibility is $\chi''(\omega) = \omega J(\omega)$. This "molecular orientation" susceptibility would be a response of the molecules to external torque and thus cannot be "measured" in a real experiment. However, several experimental techniques, such as optical Kerr effect and dielectric spectroscopy, do access response functions that are related to molecular reorientation dynamics and therefore are comparable with the "orientational" susceptibility discussed above. We therefore transform eq 6 into the susceptibility form

$$\omega/T_1 = C[\chi''(\omega) + 2\chi''(2\omega)] \equiv 3C\tilde{\chi}''(\omega) \tag{7}$$

where $\tilde{\chi}''(\omega)$ shall be called the "normalized NMR susceptibility" or simply "susceptibility". Even though it is in fact a weighted sum of two susceptibility terms, for a broad relaxation spectrum it is barely distinguishable from the individual susceptibilities, closely resembling the somewhat broadened $\chi''(2\omega)$. The factor 3 appears in order to keep the integral over the susceptibility $\tilde{\chi}''(\omega)$ normalized to $\pi/2$ as usual. As will be demonstrated, analyzing the susceptibility $\tilde{\chi}''(\omega)$ rather than the relaxation rate $1/T_1(\omega)$ itself, as is most often done in FFC NMR studies, facilitates comparisons with dielectric and mechanical spectra and spectral decompositions in terms of polymer and glassy dynamics.

The orientational correlation function $F_2(t)$ reflects segmental reorientational motion. In low molecular weight liquids, where polymer effects are absent, $F_2(t)$ probes the glassy dynamics (structural or α-relaxation). We note in passing that the characteristic "glassy dynamics" is actually established well above the melting point[3,37,38] and therefore are features of the molecular liquids in general. In these systems, the long-time end of the correlation functions (which is its only part relevant in the present context) is nonexponential. These "stretched" relaxations can be modeled with suitable phenomenological susceptibility functions[1–3,29,39] or appropriate distributions of relaxation times[40–42] (see also below).

In polymers, $F_2(t)$ contains additional contributions that reflect the characteristic and slow polymer chain dynamics, whereas its short (and main) part still reflects segmental dynamics which are identified as glassy dynamics ($\tau_\alpha = \tau_s$). At intermediate times, there remains therefore a finite correlation that cannot be relaxed by the glassy dynamics alone, as polymer connectivity and confinement effects impede full isotropic reorientation of a polymer segment. The complete relaxation is only achieved at long times in the course of Rouse and reptation dynamics. Thus, the correlation function formally becomes bimodal, although it is not a priori evident whether the "modes" are sufficiently distinct and separated in time to make their physically meaningful decomposition possible. A possible

approach to analyzing polymer dynamics is therefore to examine $F_2(t)$ at sufficiently long times (or, equivalently, $J(\omega)$ at sufficiently low frequencies), where the polymer contribution is dominant, and therefore no decomposition is necessary. Such analyses are performed in, e.g., simulation works[43,44] and in previous FFC NMR works.[14–16] However, it is not always clear how large is the contribution of the underlying glassy dynamics and whether it can be safely neglected. Another approach is thus to try to single out the different relaxation contributions and analyze them separately, as there is no "unified" theory of dynamics of polymers on all time/length scales. Here we note that this separation problem is also debated for rheological experiments.[45] As a guideline to such phenomenological decomposition, one assumes that polymer and glassy dynamics are statistically independent, so that their contributions to $F_2(t)$ are multiplicative:

$$F_2(t) = F_{\text{glass}}(t)\, F_{\text{polymer}}(t) \tag{8}$$

Depending on the molecular weight, the polymer part $F_{\text{polymer}}(t)$ may contain contributions from Rouse as well as reptation dynamics. The just presented reasoning was also used in, e.g., refs 15 and 16. Further introducing the relative magnitude f of polymer dynamics, we write

$$F_2(t) = [(1-f)\phi_{\text{glass}}(t) + f]F_{\text{polymer}}(t) \tag{9}$$

where $\phi_{\text{glass}}(t)$ denotes the normalized correlation function describing the glassy dynamics alone. It is often argued that the polymer contribution is rather small, $f = 0.001-0.01$.[15,16,22,25,46] We will show, however, later in the present study that significantly larger values of f may be observed.

B. The Dynamic Order Parameter. The relative magnitude f is related to what was called the generalized[22] or dynamic[11,24,25] order parameter S or dipolar reduction factor,[26] $f = S^2$. The parameter S is a measure of spatial restriction of the segmental motion due to the chain connectivity and confinement effects. Its meaning is somewhat related to, though different from, the orientational order parameter of nematic liquid crystals, which are characterized by long-range orientational order, i.e., static orientational order.[47] In a liquid crystal, the orientational order parameter S_{LC} reflects the degree of molecular ordering with respect to the director $\mathbf{n}$ that signifies the preferred direction in a region of the sample. It is defined through the second rank Legendre polynomial as $S_{\text{LC}} = \langle P_2(\mathbf{n}\cdot\mathbf{n}_i)\rangle$, where $\mathbf{n}_i$ is the unit orientation vector of the ith molecule. In the isotropic phase of a nematogen, S_{LC} is identically zero even in the pretransition region, even though the latter is characterized by the existence of increasingly large pseudonematic domains. One can however still introduce a local dynamic order parameter $S_{\text{LC}}(t)$ that reflects the transient (dynamic) orientational order in the space-limited domains.

Similarly, in an entangled polymer melt ($M \gg M_e$) certain segmental order within each single chain is expected on purely topological basis between the successive entanglement points, where the chain is effectively "pinned down". One can therefore introduce the local order parameter $S_{\text{loc}} = \langle P_2(\mathbf{n}\cdot\mathbf{n}_i)\rangle$, where i now only runs over the polymer segments between the entanglements, whereas $\mathbf{n}$ is the direction along the line through the entanglement points. One can further argue that, since in a melt the entanglements are not static, the local order is transient, $S_{\text{loc}} = S_{\text{loc}}(t)$ with $S_{\text{loc}}(\infty) = 0$. Experimentally, this local order in the polymer melt is difficult to access. A property that is accessible in NMR experiments is rather related to the orientational autocorrelation $F_2(t)$ that reflects correlation of a polymer segment with itself at different times. It is nevertheless true that if there exists significant orientational structural order, then the segmental reorientation is restricted to the vicinity of the local director (preferred orientation), so that the "order parameter" S, deduced from $F_2(t)$, reflects to a certain degree S_{loc}. The opposite is not necessarily true—a strong restriction of local motion per se, manifested in a large S, does not imply structural order. Indeed, imagine a glass-former where molecules are performing at short times small-angle librations in the cage formed by their neighboring molecules, and therefore S is large. This is however totally unrelated to any structural order. Therefore, due caution is needed in interpreting NMR-deduced "order parameter" S in relation to a possible local orientational order in a polymer melt. This reasoning is supported by computer simulations where indeed no significant orientational order was found although a plateau showed up in the correlation function $F_2(t)$.[43,48] Moreover, we emphasize that the way S is applied in the current context it includes both entanglement and Rouse dynamics. Finally, we note that there is certain confusion in the literature as to which quantity, $S^2 = f$ or S itself, is identified with the "dynamic order parameter". To avoid confusion, we will clearly distinguish S and f in the following.

Returning to eq 9 and assuming that the glassy and polymer dynamics are well separated in time, their relative contributions become approximately additive:

$$F_2(t) \simeq (1-S^2)\phi_{\text{glass}}(t) + S^2 F_{\text{polymer}}(t) \tag{10}$$

In such eventuality, the glassy and polymer contributions to the NMR susceptibility are likewise additive:

$$\tilde{\chi}''(\omega) = (1-S^2)\tilde{\chi}''_{\text{glass}}(\omega) + S^2\tilde{\chi}''_{\text{polymer}}(\omega) \tag{11}$$

The squared order parameter S^2 is then given by the relative integrated intensity of the polymer contribution:

$$S_2 = f = \int_{-\infty}^{\infty}\tilde{\chi}''_{\text{polymer}}(\omega)\, \mathrm{d}\ln\omega \Big/ \int_{-\infty}^{\infty}\tilde{\chi}''(\omega)\, \mathrm{d}\ln\omega \tag{12}$$

where is $\bar{\chi}''(\omega)$ the measured non-normalized total NMR susceptibility spectrum. Equation 11 indicates that the total spectrum resembles the spectrum of polymer dynamics only when the latter dominates, $(1-S^2)\tilde{\chi}''_{\text{glass}}(\omega) \ll S^2\tilde{\chi}''_{\text{polymer}}(\omega)$. Since S^2 is small (though larger than expected), this condition is not fulfilled in general. Consequently, interpreting relaxation data of polymers without accounting for the underlying glass spectrum may be misleading. In the present contribution we will identify $\bar{\chi}''_{\text{glass}}$, which we will use to separate $\bar{\chi}''_{\text{polymer}}$ from the overall susceptibility data. In paper II the polymer contribution $\bar{\chi}''_{\text{polymer}}$ will be analyzed in terms of the Rouse dynamics.

C. Analysis of the Dielectric Spectra. Our present analysis of FFC NMR spectra relies on the possibility to obtain the time constants of the glassy dynamics (i.e., of local segmental motion) by alternative means, namely by dielectric spectroscopy (DS).[2,3,29] In the case of polymers, it is only when the monomeric dipole moment has a finite component along the chain, as in the so-called "type A" polymers in Stockmayer's classification,[28] that the dielectric spectrum reflects polymer dynamics in the form of a "normal mode".[28,29] However, most polymers, including PB, are of "type B", with a vanishing dipole moment along the chain. DS is then insensitive to the chain dynamics and only detects local segmental motions (glassy dynamics), so that one can extract the time constant of the latter $\tau_s(T) = \tau_\alpha(T)$. Accordingly, dielectric spectra of high molecular weight PB were studied by different groups.[49,50] It was in particular found that the time constants agree with those from ^{2}H NMR studies,[51] the latter reflecting local segmental dynamics. In addition, a molecular dynamics study[52] explicitly showed that the dielectric relaxation probes local reorientations on the segmental length scale.

Dielectric relaxation of molecular liquids and polymers invariably exhibits stretched, nonexponential behavior. Such nonexponential relaxation can be formally described with a suitable distribution of relaxation times $G(\ln\tau)$, so that the

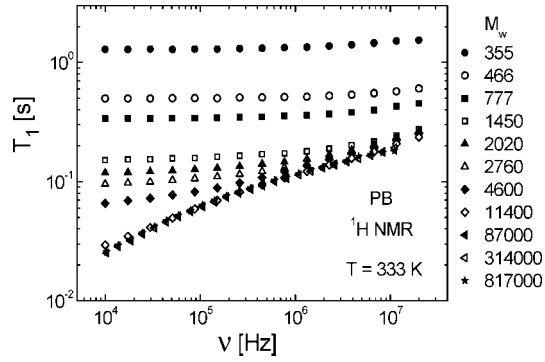

Figure 1. Spin−lattice relaxation time T_1 as a function of frequency ν of a series of 1,4-polybutadienes (PB) with different molecular weights M (weight-average, as indicated) at the same temperature $T = 333$ K.

complex dielectric permittivity $\hat{\varepsilon}(\omega)$ is obtained by integrating individual Debye contributions:

$$\hat{\varepsilon}(\omega) - \varepsilon_\infty = \Delta\varepsilon \int_{-\infty}^{\infty} G(\ln \tau) \frac{1}{1 + i\omega\tau} \, \mathrm{d} \ln \tau \qquad (13)$$

Several equally suited phenomenological distribution functions $G_\alpha(\ln \tau)$ were proposed for describing the main α relaxation.[1,29,39] We choose the generalized gamma (GG) distribution that allows to describe α-relaxation shapes with a small number of fitting parameters.[40–42,49] Our model distribution of relaxation times thus reads

$$G_\alpha(\ln \tau) = N(\alpha, \beta) \mathrm{e}^{(-\beta/\alpha)(\tau/\tau_0)^\alpha} \left(\frac{\tau}{\tau_0}\right)^\beta \qquad (14)$$

with

$$N(\alpha, \beta) = \left(\frac{\beta}{\alpha}\right)^{\beta/\alpha} \alpha / \Gamma\left(\frac{\beta}{\alpha}\right) \quad \text{and} \quad \tau_\alpha = \tau_0 \left(\frac{\alpha}{\beta}\right)^{1/\alpha} \frac{\Gamma\left(\frac{\beta+1}{\alpha}\right)}{\Gamma\left(\frac{\beta}{\alpha}\right)} \qquad (15)$$

The susceptibility functions derived from the GG distribution are rather similar to those of the Kohlrausch stretched exponential $\phi_{\mathrm{glass}}(t) = \exp[-(t/\tau_K)^{\beta_K}]$.[41] We found that the Kohlrausch function provides a somewhat better interpolation of the data of the liquids *o*-terphenyl and tristyrene. PB exhibits a secondary relaxation peak (β-process) in the kHz−MHz range,[49,50] which also has to be accounted for in the spectral analysis (see Figure 2). We interpolated the β-peak with a symmetric distribution of relaxation times,[2,41,49] using the so-called Williams−Watts approach.[53] Details of this analysis, irrelevant for the present determination of time constant τ_α, can be found in refs 41 and 49.

III. Experimental Part

The dispersion of the spin−lattice relaxation time T_1 was determined with a STELAR relaxometer FFC 2000,[16] which allows measurements in the temperature range of 200− 390 K. At each temperature setting of the instrument, we ran the complete set of PB samples in order to ensure consistent temperatures between the samples. The accuracy of temperature measurements was better than ±1 K, while the temperature stability better than ±0.3 K. For temperature control, we used a thermocouple in a probe tube, inserted into the probe head at the sample position. We observed simple exponential relaxation of magnetization over at least 1 order of magnitude in magnetization and thus determined the time constant T_1 by fitting to the exponential function.

Broad-band dielectric measurements were carried out with a Schlumberger SI 1260 phase gain amplifier together with a BDC current-to-voltage converter from Novocontrol.[49] This setup covers a frequency range of 10^{-2}−10^7 Hz. The glass transition was identified at a temperature T_g, where the dielectric time constant equals 100 s. Dielectric data and T_g of *o*-terphenyl and tristyrene are reported in refs 54 and 55.

Standard 1,4-polybutadiene (PB) samples with low polydispersity, as well as tristyrene, were purchased from Polymer Standards Service (PSS), Mainz, Germany (also those provided by S. Stapf, cf. Acknowledgment). The concentrations of cis, trans, and vinyl units were determined for some of the samples.[27] The trans content is always close to 50%, and the vinyl content decreases from about 20% at $M \cong 1000$ to about 6% beyond $M \cong 10\,000$. The glass-former *o*-terphenyl (OTP; 99% purity) was obtained from Aldrich. Table 1 lists the samples and their properties. All the samples were degassed on a vacuum line, filled into 10 mm diameter test tubes, and thereafter annealed. Throughout the paper, we use weight-averaged mass M_w to specify the molecular weight M of the samples.

IV. Results

A. Polymer and Glassy Dynamics. In the present study, we measured the frequency and temperature dependence of the ^{1}H NMR spin−lattice relaxation time T_1 of a series of 1,4-polybutadienes (PB), covering a broad range of molecular weights M from 355 to 817 000 g/mol. Included in the study are PB with the lowest M that still could be characterized avoiding crystallization. Table 1 lists the samples and their properties. The aim of the study is investigating the crossover from simple liquid dynamics to Rouse and finally to entanglement dynamics. In Figure 1, the relaxation time T_1 for a single temperature $T = 333$ K is presented as a function of frequency ν in the range of 10 kHz ≤ ν ≤ 20 MHz that is covered by our fast field cycling (FFC) NMR instrumentation. It is seen in Figure 1 that the lowest M systems exhibit virtually no dispersion of T_1, which is typical of simple liquids at high temperatures relative to T_g. Dispersion appears, however, with increasing M. At $M \geq 11\,400$, the dispersion does not change with further increasing M, which implies that at this M the system reaches the limiting behavior as expected for a fully entangled melt.

As discussed, dynamics of a polymer comprises characteristic collective chain dynamics and (usually dominant) local segmental motion, the latter belonging to the glass transition phenomenon (see section II). We remind the reader that we use the term "polymer dynamics" to refer exclusively to the polymer-specific part and call the rest "glassy dynamics". Since in polymers local segmental dynamics actually represents α-relaxation, the segmental time scale is the one of α-relaxation, $\tau_s \cong \tau_\alpha$. It is a well-known fact that the segmental dynamics slows down with increasing molecular weight; accordingly, the glass transition temperature T_g increases, until a saturation is reached at high M.[10,56,57] Thus, the dispersion effects observed in Figure 1 are due to changes of both chain and glassy dynamics with increasing M.

The time constants $\tau_\alpha(T)$ can be obtained from independent dielectric experiments, which in the case of PB are insensitive to the polymer chain dynamics (see section II). Typical dielectric spectra of PB with a low and high molecular weight are shown in Figure 2, whereas the dielectric time constants $\tau_\alpha(T)$ of all samples, obtained from fits to the GG function (eqs 14 and 15) with $\alpha = 0.33$ and $\beta = 0.5$−0.6, are displayed in Figure 3. We note that, due to the low dipole moment of PB, the dielectric permittivity is rather small, so that the spectra exhibit visible noise. Still, there is clearly only a single α-relaxation peak and no sign of a normal mode at lower frequencies, which is an expected behavior of a type B polymer. However, at higher frequencies there is a secondary relaxation peak, which also has to be accounted for in the fitting procedure at low temperatures close to T_g (full line). At high temperatures, only

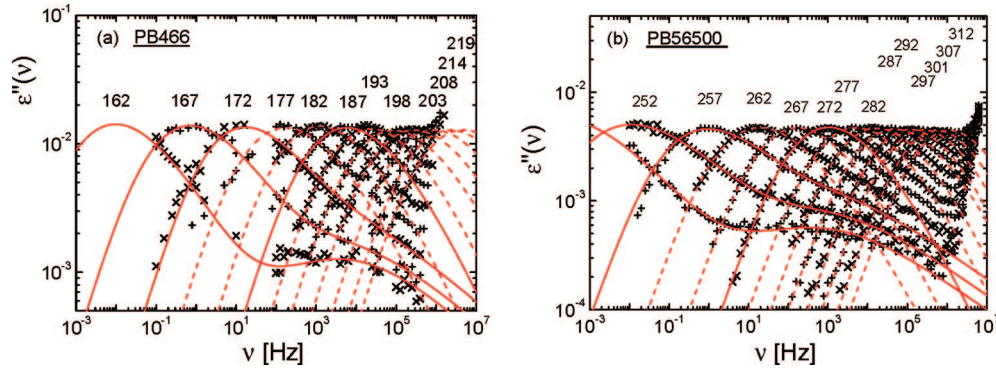

Figure 2. Dielectric spectra of the polybutadiene samples PB466 (a) and PB56500 (b) (numbers indicate temperature in K): full lines, fits to the generalized gamma distribution of relaxation times for the α-peak (eq 14) plus a suitable distribution for the β-process; dashed lines, α-parts fit only.

Table 1. Details of the Measured *o*-Terphenyl (OTP), Tristyrene, and 1,4-Polybutadiene (PB) Samples[a]

name	M_w [g/mol]	M_n [g/mol]	M_w/M_n	T_g [K]
PB355	355	335	1.06	140.9
PB466	466	437	1.06	161.2
PB777	777	732	1.06	165.3
PB1450	1450	1350	1.08	170.7
PB2020	2020	1890	1.07	173.6
PB2760	2760	2640	1.05	174.4
PB4600	4600	4470	1.03	174.0
PB56 500	56500	55500	1.02	
PB87 000	87000	86000	1.01	174.4
PB314 000	314000	308000	1.02	
PB817 000	817000	774000	1.05	
OTP				244.0
tristyrene				233.0

[a] Note that the name of the PB samples reflects its molecular weight M_w. Systems for which T_g is reported were also measure by dielectric spectroscopy.

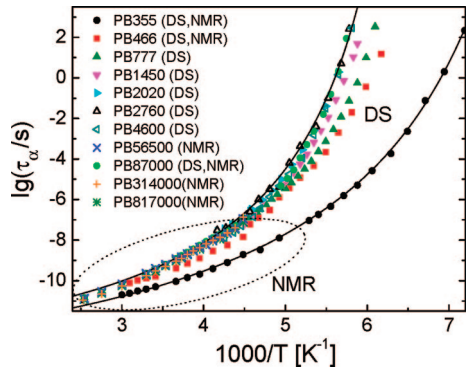

Figure 3. Time constants of the α-process (segmental relaxation) of the 1,4-polybutadienes (PB) samples with indicated molecular weight as obtained by analyzing the dielectric spectra (DS) and the FFC NMR spectra (the latter marked with ellipse); solid lines: interpolations with the Vogel−Fulcher−Tammann equation.

the main relaxation peak is fitted (dashed line). In any case, the relaxation time $\tau_\alpha(T)$ is accurately obtained by only fitting the α-peak maximum and its low-frequency wing, so that we do not expect any significant errors in the deduced $\tau_\alpha(T)$ due to the presence of a secondary relaxation. Inspecting Figure 3, one recognizes a non-Arrhenius behavior of the time constants, typical of glass-forming systems. Below $M \cong 2020$, the time constants become M-dependent, which means that not only the polymer but also the glassy dynamics sensitively depend on M in the molecular weight range in which one expects a crossover from simple liquid dynamics to the polymer one, described by Rouse theory.

B. Dispersion in Low Molecular Weight Glass-Formers. In order to disentangle chain and segment dynamics, we first investigated the dispersion behavior of simple liquids where no polymer effects are present. Though numerous NMR relaxation studies on simple liquids are found in the literature,[13,58–66] we are not aware of any systematic FFC NMR work that exploits the full strength of STELAR spectrometer and covers the supercooled state. As such reference system, we chose the glass-former *o*-terphenyl (OTP), which we characterized in the temperature range 263 K ≤ T ≤ 393 K (T_g = 243 K). The corresponding relaxation times $T_1(\nu)$ are plotted in Figure 4a, whereas the NMR susceptibility $\bar{\chi}''(\nu) \propto \nu/T_1(\nu)$ in Figure 4b. In the susceptibility representation, the relaxation data show similarity with the dielectric loss spectra. At 296 K, a maximum first appears on cooling. We interpret the maximum as due to the main α-relaxation. Note that FFC NMR allows covering more than 3 decades to lower frequencies from the relaxation maximum, whereas in dielectric spectra this frequency range is usually obscured by parasitic conductivity contribution. Thus, a particular strength of NMR relaxometry lies in its ability to access dynamic processes with low spectral densities, which are much slower than the main relaxation. In contrast to polymer melts, such slow processes are absent in simple liquids, so that the low-frequency ($\omega\tau_\alpha \ll 1$) susceptibility is linear in frequency $\bar{\chi}''(\nu) \propto \nu$. This corresponds to the "extreme narrowing" condition with a constant $T_1(\omega)$ (see, e.g., Figure 4a).

For T = 296 K and T = 303 K, the susceptibility spectra show a discernible relaxation maximum (cf. Figure 4b). They were thus fitted to the Kohlrausch function to determine the time constant τ_α and stretching parameter $\beta_K = 0.61$. Then, the susceptibility is plotted as a function of the reduced frequency $\omega\tau_\alpha$. For all the other temperatures, we assume the validity of the frequency−temperature superposition (FTS) and shift the spectra horizontally without altering their relative amplitudes, until they join up with each other and with the 296 and 303 K spectra discussed above. The master curve of OTP, shown in Figure 5, is well interpolated with the Kohlrausch function (red line).

Applying FTS is a crucial point of our analysis. The FTS principle implies that the shape of the susceptibility spectra is not changing with the temperature. Usually, FTS holds rather well in supercooled liquids, especially at higher temperatures[1–3,67,68] though it may fail at low temperatures close to T_g.[2,3,38,69,70] Indeed, at the lowest temperatures we find a slight change of amplitude of the susceptibility maximum with temperature, actually too small to be discernible in the logarithmic plot of Figure 4b, but nevertheless indicating that the stretching parameter β may slightly change. However, most of the NMR data are analyzed at much higher temperatures well above T_g. Moreover, the time constants $\tau_\alpha(T)$, obtained from

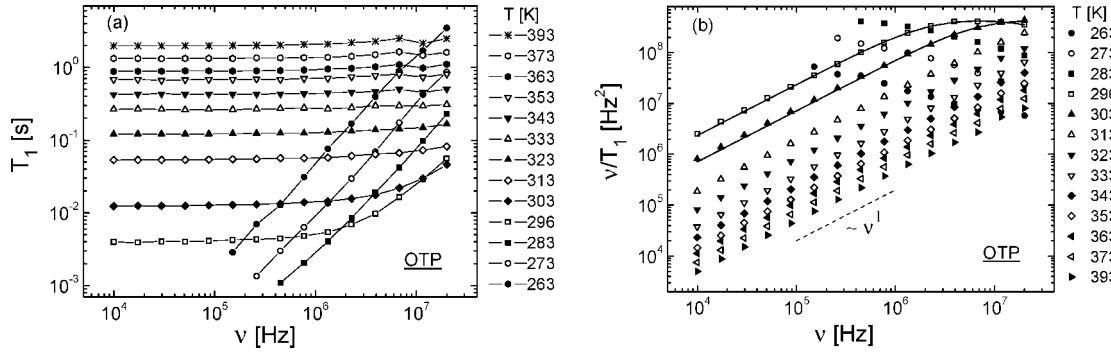

Figure 4. (a) Spin−lattice relaxation time T_1 of the glass former *o*-terphenyl (OTP) as a function of frequency ν; solid lines: guides to the eye. (b) Relaxation data of (a) in the susceptibility representation $\bar{\chi}''(\nu) \propto \nu/T_1(\nu)$ (cf. eq 7); solid lines: interpolations with a Kohlrausch susceptibility with the stretching parameter $\beta_K = 0.61$; dashed line indicates linear behavior of simple liquids (Debye behavior).

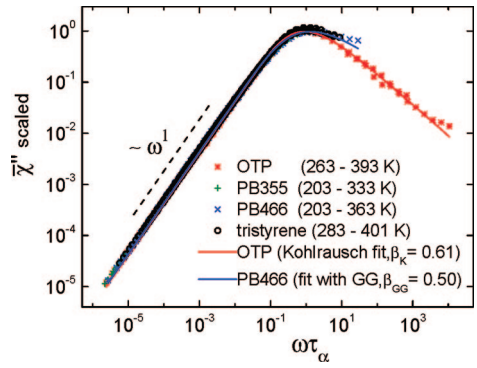

Figure 5. Master curves of the susceptibility resulting from applying temperature−frequency superposition for *o*-terphenyl (OTP), tristyrene, and the two low molecular weight 1,4-polybutadienes PB355 and PB466. Lines: corresponding interpolations with the generalized gamma distribution (GG) and Kohlrausch function.

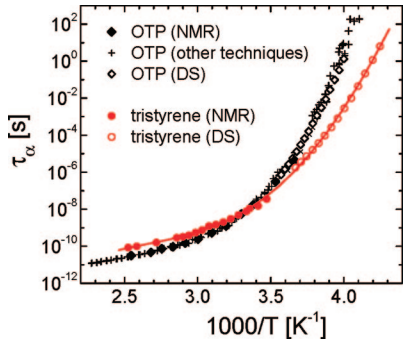

Figure 6. Time constants of the main relaxation in *o*-terphenyl (OTP) and tristyrene as obtained by FFC NMR and by dielectric spectroscopy (DS)[55] and other techniques.[3,61,65] Solid line for tristyrene presents a fit to the Vogel−Fulcher−Tammann law.

constructing the master curve in Figure 5, agree well with those reported for OTP by other techniques,[3,55,61,65] as is shown in Figure 6. Four decades of correlation times are covered by NMR, from 10^{-11} s $< \tau_\alpha(T) < 10^{-7}$ s. Thus, we conclude that FTS works sufficiently well at high temperatures where the FFC NMR data are collected. Independent of the applied methods, the corresponding time constants reflecting reorientational dynamics are virtually identical and show a super-Arrhenius temperature dependence which is, as said, typical of supercooled liquids.

Next, we investigated the oligomers PB355 and PB466 as well as tristyrene. Some NMR susceptibility data are shown in Figure 7. The spectra of PB that exhibit a maximum are interpolated by the GG distribution with $\alpha = 1$ and $\beta_{GG} = 0.50$, whereas tristyrene spectra by the Kohlrausch function ($\beta_K =$ 0.55). The data were then replotted as functions of $\omega\tau_\alpha$. Accounting for different coupling constant C, each master curve is vertically shifted to agree at the maximum and included in Figure 5, while the time constants are shown in Figures 3 (PB) and 6 (tristyrene). We note that within the accuracy of the experimental data the height of relaxation maximum of all the PB samples is M-independent. All master curves perfectly agree at $\omega\tau_\alpha < 1$, whereas at $\omega\tau_\alpha > 1$ they go apart predominantly due to the different relaxation stretching. Included in Figure 5 is an interpolation of the PB466 data with the GG distribution, which provides an adequate fit.

In the following analysis of the emerging polymer dynamics, we are only interested in the frequency range $\omega\tau_\alpha < 1$, where this dynamics appears. We note that the systems of Figure 5 do not exhibit any additional intensity in this range in excess of $\bar{\chi}''(\omega) \propto \omega$ and thus do not show polymer dynamics. While this conclusion is quite obvious for OTP, it also means that the oligomers PB355 and PB466 as well as tristyrene are not "polymers" yet. We shall call this behavior the simple liquid limit. Inspecting their temperature dependence of τ_α, obtained when constructing master curves, with the dielectric ones (cf. Figures 3 and 6) again shows that both time constants agree well. More than 12 decades of correlation times are covered by combining FFC NMR relaxation and dielectric data.

C. High Molecular Weight 1,4-Polybutadiene. We show in Figure 8 the NMR susceptibility data of PB56500, i.e., a relatively high molecular PB. Now, the low-frequency part is not linear in frequency any longer but exhibits an excess intensity over $\bar{\chi}''(\omega) \propto \omega$. These new spectral features are attributed to the polymer chain dynamics. This behavior is well recognized when the master curve of PB56500 is compared with those of low molecular weight PB liquids, as seen in Figure 9. The susceptibility curves of higher molecular weight samples can no longer be analyzed in terms of a GG distribution of relaxations times, as there are now additional relaxation features on the low-frequency side of the α-peak due to the emerging polymer dynamics. We assume, however, based on the dielectric spectral shapes (see paper II), that the glassy dynamics, mostly pronounced at the relaxation maximum, are rather similar for different M. Thus, in order to compare the high and low molecular weight spectra, we plot each in Figure 9 against the reduced frequency $\omega\tau_\alpha$, so that they overlap at $\omega\tau_\alpha \geq 1$, where the polymer dynamics are absent. The difference between the polymer and low molecular weight spectra at $\omega\tau_\alpha < 1$ is then identified with the polymer dynamics alone (see eq 11 and Figure 9). The data of the samples PB87000, PB314000, and PB817000, all coincide with those of PB56500, and the corresponding master curves are included in Figure 9. Also, the time constants $\tau_\alpha(T)$ agree as is seen from Figure 3. We hence conclude that for $M \geq 56\,500$ the polymer dynamics in

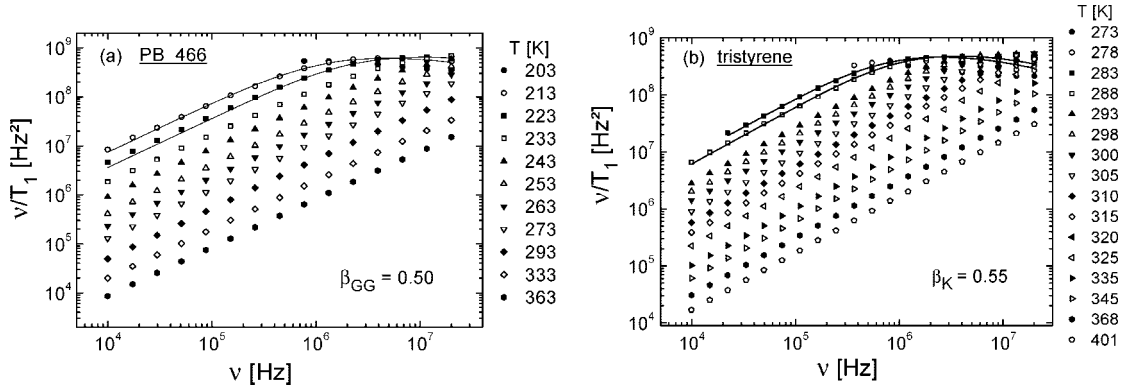

Figure 7. FFC NMR susceptibility data of 1,4-polybutadiene (PB) with $M = 466$ (a) and of tristyrene (b). The spectra showing a maximum are interpolated (solid lines) with the generalized gamma distribution (PB) and Kohlrausch function (tristyrene).

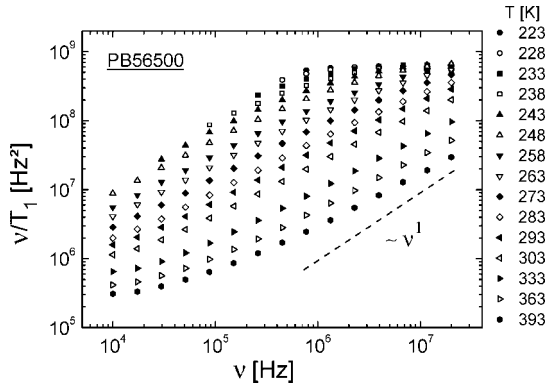

Figure 8. NMR relaxation data of 1,4-polybutadiene (PB) with $M = 56\,500$ in the susceptibility representation.

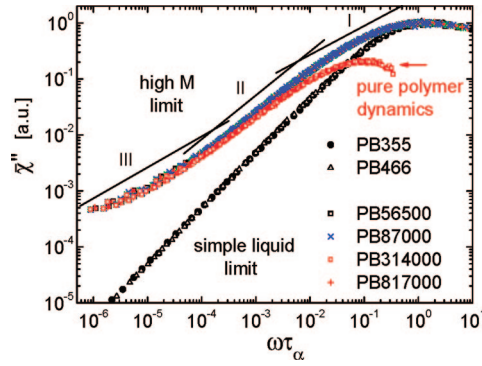

Figure 9. Master curves for the susceptibility as a function of the scaled frequency $\omega\tau_\alpha$ for high molecular weight 1,4-polybutadienes (PB) as indicated and for the low molecular weight polybutadienes. The difference (red) between the high and low molecular weight spectra for PB817000 is identified with pure polymer dynamics. Straight lines indicate power-law regimes (I, II, and III) as discussed by Kimmich and co-workers.[15,16]

the intermediate or "mesoscopic" frequency range of Figure 9 is *M*-independent, having thus reached its high-*M* limit, whereas the still developing reptation dynamics is too slow to be fully resolved in the accessible frequency window. Concentrating on the "pure" polymer spectrum in Figure 9, obtained by subtracting the spectrum of glassy dynamics from the total (eq 11), its relative integrated intensity (eq 12) is $f = 0.11$, corresponding to a surprisingly high dynamic order parameter $S = 0.34$.

V. Discussion and Conclusions

All investigated low molecular weight liquids, namely *o*-terphenyl, tristyrene, PB355, and PB466, exhibit highly similar FFC NMR susceptibility in the frequency range $\omega\tau_\alpha \leq 1$. The resulting master curves cover about 7 decades in frequency and 5 decades in intensity at $\omega\tau_\alpha \ll 1$. This broad dynamic range makes FFC NMR well suited to probe dynamic processes that are slower than the main relaxation in a liquid, for example, the collective chain dynamics in polymer melts. Usually, such low frequencies are not accessible to dielectric spectroscopy (DS) because of parasitic dc conductivity. Moreover, most polymers are of type B, so that the dielectric spectra only reflect segmental dynamics governed by the glass process. On the other hand, this feature of DS can be considered advantageous, as it allows us to check whether the segmental correlation times, extracted under the assumption of FTS from the present analysis of the NMR spectra, agree with those from DS. In fact, we found such agreement, which justifies our use of FTS. As in the case of mechanical spectra,[4–6] applying FTS is equivalent to covering a significantly broader range of frequencies than a single measurement can access. Examining the temperature dependence of relaxation time, we found that both the FFC NMR and DS time constants show a non-Arrhenius behavior typical of glass-forming systems. The NMR time constants cover a broad range of 10^{-11}–10^{-7} s.

The oligomers PB355 and PB466, as well as tristyrene, do not show any sign of collective chain dynamics, e.g., no onset of Rouse modes, yet. The Rouse unit M_R must then be larger than say 500. The susceptibility spectra of these systems are quite similar to the permittivity spectra collected by DS. At low frequencies, all the NMR spectra of the low molecular systems exhibit a linear behavior $\tilde{\chi}''(\omega) \propto \omega$, typical of simple liquids. It appears that the linear structure of (flexible) chains is immaterial for the relaxation dynamics, the latter resembling the behavior even of the monomeric glass-former *o*-terphenyl. In contrast, the four high molecular weight polymers (PB56500–PB817000) show a different spectral pattern. A significant contribution in excess of ω^1 is observed at $\omega\tau_\alpha < 1$, which is associated with the polymer chain dynamics. The virtues of FFC NMR in accessing polymer dynamics are thus evident. In terms of the segmental reorientation correlation function, the relatively fast dynamics of the α-process does not lead to a complete loss of correlation (isotropization), but rather leaves certain residual correlation that only decays at much longer times $t \gg \tau_\alpha$ in the course of Rouse and reptation dynamics. This final decay corresponds to a contribution in the NMR susceptibility, which is much weaker than the main relaxation maximum, the latter due to local segmental motion. Such low signal levels can be hardly detected with adequate precision by most other techniques.

The dispersion data $T_1(\omega)$ of the high molecular weight PB agree well with that reported by Kimmich et al.[33,71] Analyzing T_1 dispersion data of several polymers, Kimmich and Fatkul-

lin[15,16,72] identified three power law regimes (I−III) in the frequency range $\omega\tau_\alpha \ll 1$ and discussed them in terms of the model of renormalized Rouse modes.[73] We show these power laws in Figure 9. Indeed, in fair approximation they describe the low-frequency side of the master curve for the high-*M* PB systems. However, regime I is already very close to the susceptibility maximum, where the ever-present contribution of glassy dynamics strongly affects the spectral shape. Moreover, the power law I is almost impossible to identify, as the master curve is continuously curved in the corresponding frequency range. The polymer dynamics has thus to be separated from the total spectrum prior to analyses. This can be achieved, e.g., by assuming that different contributions are approximately additive (eq 11) and subtracting the glassy dynamics spectrum (taken from the FFC NMR spectra of the low-*M* PB) from the full relaxation spectrum (cf. Figure 9).

Clearly, the spectrum of polymer dynamics alone is quite different from the total one. In particular, the power law regimes I and II do not appear any longer. According to eq 11, we argue that only if $(1 - S^2)\tilde{\chi}''_{\mathrm{glass}}(\omega) \ll S^2\tilde{\chi}''_{\mathrm{polymer}}(\omega)$ do the overall dispersion data reflect polymer dynamics alone. Thus, in cases in which $f = S^2$ is small as in PB, even at frequencies significantly below the relaxation maximum there is a non-negligible contribution of glassy dynamics in the spin−lattice relaxation rate $1/T_1(\omega)$. In other words, separation of time scales of polymer and glassy dynamics is not sufficient to argue that the polymer dynamics makes a dominant contribution in its frequency range. As will be shown in paper II, this is especially true for low molecular weight PB samples exhibiting only Rouse dynamics due to their particularly small *S*. More generally, we believe that in most complex liquids, studied by FFC NMR or other techniques, a relatively fast main relaxation process has to be taken into account in addition to the slow and weak low frequency dynamics.[74] Returning to different regimes of polymer dynamics and their characteristic power laws, discussed above, we believe that, unless the underlying α-relaxation is properly accounted for, the apparent power law exponents do not, in fact, reflect the actual polymer dynamics and therefore lack the intended significance. In particular, no universal dynamics is expected to be observed in the total relaxation FFC spectra since the value of *S* depends on the choice of the proton spin pairs via which polymer dynamics is monitored[24,25] (cf. below and paper II).

The isolated "polymer spectra" may be interpreted in terms of Rouse dynamics, entanglement effects, and the concomitant reptation dynamics, which will be subject of paper II. Here, we only mention that the main contribution around the maximum of the polymer spectrum down to $\omega\tau_\alpha \approx 10^{-4}$ in Figure 9 will be attributed to Rouse dynamics whereas the reptation dynamics only give a minor contribution at the lowest accessible frequencies.

Examining the spectra of the high molecular weight PB, we find that the relative relaxation strength of polymer chain dynamics is $f = S^2 = 0.11$, which corresponds to a dynamic order parameter of $S = 0.34$. This is a rather high value. Usually, it is argued that S^2 in polymers is small, $S^2 = 0.001-0.01$.[15,25] Dollase et al.[25] pointed out, as said before, that the experimental *S* depends on the internuclear vector that is probed in the experiment. Indeed, applying double-quantum NMR, which allows to select different spin pairs in the monomer unit, quite different order parameters were reported; however in all cases again rather high, $S = 0.1-0.2$. This is close to our results. However, we have to keep in mind that an order parameter $S = 0.34$ of the present study includes the effect of both Rouse and reptation dynamics whereas Dollase et al. attribute their findings solely to entanglement effects. We reiterate this point in paper II.

Acknowledgment. The authors thank S. Stapf for supplying the high molecular weight polybutadiene samples ($M = 56\,500$, 87 000, 314 000, and 817 000). Fruitful discussions with N. Fatkullin are appreciated. Support of Deutsche Forschungsgemeinschaft (DFG) through SFB 481 is highly acknowledged.

References and Notes

(1) Angell, C. A.; Ngai, K. L.; McKenna, G. B.; McMillan, P. F.; Martin, S. W. *J. Appl. Phys.* **2000**, *88*, 3113–3157.
(2) Lunkenheimer, P.; Schneider, U.; Brand, R.; Loidl, A. *Contemp. Phys.* **2000**, *41*, 15–36.
(3) Blochowicz, T.; Brodin, A.; Rössler, E. A. *Adv. Chem. Phys.* **2006**, *133*, 127–256.
(4) Ferry, J. D. *Viscoelastic Properties of Polymers*, 3rd ed.; Wiley: New York, 1980.
(5) Doi, M.; Edwards, S. F. *The Theory of Polymer Dynamics*; Oxford Sci. Publication: New York, 1986.
(6) McLeish, T. C. B. *Adv. Phys.* **2002**, *51*, 1379–1527.
(7) Gray, R. W.; Harrison, G.; Lamb, J. *Proc. R. Soc. London* **1977**, *356*, 77–102.
(8) Majeste, J.-C.; Montfort, J.-P.; Allal, A.; Marin, G. *Rheol. Acta* **1998**, *37*, 486–499.
(9) Mondello, M.; Grest, G. S.; Webb III, E. B.; Peczak, P. *J. Chem. Phys.* **1998**, *109*, 798–805.
(10) Ding, Y.; Kisliuk, A.; Sokolov, A. P. *Macromolecules* **2004**, *37*, 161–166.
(11) (a) Kariyo, S.; Gainaru, C.; Schick, H.; Brodin, A.; Novikov, V. N.; Rössler, E. A. *Phys. Rev. Lett.* **2006**, *97*, 207803-1–207803-4. (b) Erratum: Kariyo, S.; Herrmann, A.; Gainaru, C.; Schick, H.; Brodin, A.; Novikov, V. N.; Rössler, E. A. *Phys. Rev. Lett.* **2008**, *100*, 109901–1.
(12) Jacobsson, P.; Börjesson, L.; Torell, L. M. *J. Non-Cryst. Solids* **1991**, *131−133*, 104–108.
(13) Noack, F. *Prog. NMR Spectrosc.* **1986**, *18*, 171–276.
(14) Kimmich, R. *Chem. Phys.* **2002**, *284*, 253–285.
(15) Kimmich, R.; Fatkullin, N. *Adv. Polym. Sci.* **2004**, *170*, 1–113.
(16) Kimmich, R.; Anoardo, E. *Prog. NMR Spectrosc.* **2004**, *44*, 257–320.
(17) Rachocki, A.; Kowalczuk, J.; Tritt-Goc, J. *Solid State Nucl. Magn. Reson.* **2006**, *30*, 192–197.
(18) Doi, M. In *Material Science and Technology*; Verlag Chemie: Weinheim, Vol. *12*, p 389.
(19) Cho, K. S.; Ahn, K. H.; Lee, S. J. *J. Polym. Sci., Part B: Polym. Phys.* **2004**, *42*, 2724–2729.
(20) Liu, C.; He, J.; Keunings, R.; Bailly, C. *Macromolecules* **2006**, *39*, 3093–3097.
(21) Klein, P. G.; Adams, C. H.; Brereton, M. G.; Ries, M. E.; Nicholson, T. M.; Hutchings, L. R.; Richards, R. W. *Macromolecules* **1998**, *31*, 8871–8877.
(22) Cohen-Addad, J. P. *J. Chem. Phys.* **1975**, *63*, 4880–4885.
(23) Lipari, G.; Szabo, A. *J. Am. Chem. Soc.* **1982**, *104*, 4546–4559.
(24) Graf, R.; Heuer, A.; Spiess, H. W. *Phys. Rev. Lett.* **1998**, *80*, 5738–5741.
(25) Dollase, T.; Graf, R.; Heuer, A.; Spiess, H. W. *Macromolecules* **2001**, *34*, 298–309.
(26) Callaghan, P. T.; Samuski, E. T. *Macromolecules* **2000**, *33*, 3795–3802.
(27) Lusceac, S. A.; Gainaru, C.; Vogel, M.; Medick, P.; Koplin, C.; Rössler, E. A. *Macromolecules* **2005**, *38*, 5625–5633.
(28) Stockmayer, W. H. *Pure Appl. Chem.* **1967**, *15*, 539–554.
(29) Kremer, F., Schönhals, A., Eds. *Broadband Dielectric Spectroscopy*; Springer: Berlin, 2003.
(30) Lindner, P.; Rössler, E.; Sillescu, H. *Makromol. Chem.* **1981**, *182*, 3653–3669.
(31) Sholl, C. A. *J. Phys. C* **1981**, *14*, 447–464.
(32) Kehr, M.; Fatkullin, N.; Kimmich, R. *J. Chem. Phys.* **2007**, *126*, 094903-1–094903-8.
(33) Kimmich, R.; Fatkullin, N.; Seitter, R. O.; Gille, K. *J. Chem. Phys.* **1998**, *108*, 2173.
(34) Abragam, A. *The Principles of Nuclear Magnetism*; Clarendon Press: Oxford 1961.
(35) Blochowicz, Th.; Kudlik, A.; Benkhof, S.; Senker, J.; Rössler, E.; Hinze, G. *J. Phys. Chem.* **1999**, *110*, 12011–12022.
(36) Bloembergen, N.; Purcell, E. M.; Pound, R. V. *Phys. Rev.* **1948**, *73*, 679–715.
(37) Wiebel, S.; Wuttke, J. *New J. Phys* **2002**, *4*, 56.156.17.
(38) Brodin, A.; Rössler, E. A. *J. Phys.: Condens. Matter* **2006**, *18*, 8481–8492.
(39) Böttcher, C. J. F.; Borderwijk, P. *Theory of Electric Polarization*, 2nd compl. rev. ed.; Elsevier: Amsterdam, 1978; Vol. *2*.
(40) Nicolai, T.; Gimel, J. C.; Johson, R. *J. Phys. II* **1996**, *6*, 697–711.

(41) Blochowicz, Th.; Tschirwitz, Ch.; Benkhof, St.; Rössler, E. A. *J. Chem. Phys.* **2003**, *118*, 7544–7555.
(42) Blochowicz, T.; Gainaru, C.; Medick, P.; Tschirwitz, C.; Rössler, E. A. *J. Chem. Phys.* **2006**, *124*−1−11.
(43) Faller, R.; Müller-Plathe, F.; Heuer, A. *Macromolecules* **2000**, *33*, 6602–6610.
(44) Kreer, T.; Baschnagel, J.; Müller, M.; Binder, K. *Macromolecules* **2001**, *34*, 1105–1117.
(45) Roland, M. C.; Archer, L. A.; Mott, P. H.; Sanches-Reyes, J. *J. Rheol.* **2004**, *48*, 395–403.
(46) Kuhn, W.; Grün, F. *Kolloid Z.* **1942**, *101*, 248–271.
(47) Demus, D., Goodby, J., Gray, G. W., Spiess, H. W., Vill, V., Eds. *Handbook of Liquid Crystals*; Wiley VCH: New York, 1998.
(48) Faller, R.; Kolb, A.; Müller-Plathe, F. *Phys. Chem. Chem. Phys.* **1999**, *1*, 2071–2076.
(49) Kudlik, A.; Benkhof, S.; Tschirwitz, T.; Blochowicz, T.; Rössler, E. *J. Mol. Struct.* **1999**, *479*, 201–218.
(50) Deegan, R. D.; Nagel, S. R. *Phys. Rev. B* **1995**, *52*, 5653–5656.
(51) Rössler, R.; Sokolov, A. P.; Warschewske, U.; Eiermann, P. *Physica A* **1993**, *201*, 237–256.
(52) Smith, G. D.; Borodin, O.; Paul, W. *J. Chem. Phys.* **2002**, *117*, 10350–10359.
(53) Williams, G.; Watts, D. C. *Trans. Faraday Soc.* **1970**, *66*, 80–85.
(54) Blochowicz, T. PhD Thesis, University of Bayreuth, **2003**.
(55) Richert, R. *J. Chem. Phys.* **2005**, *123*−1−3.
(56) Fox, T.; Flory, P. J. *J. Polym. Sci.* **1954**, *14*, 315–319.
(57) Ueberreiter, K.; Kanig, G. *J. Colloid Sci.* **1952**, *7*, 569–583.
(58) McCall, D. W.; Douglas, D. C.; Falcone, D. R. *J. Chem. Phys.* **1969**, *50*, 3839–3843.
(59) Noack, F.; Preissing, G. *Z. Naturforsch.* **1969**, *A24*, 143–153.
(60) Rössler, E.; Sillescu, H. *Chem. Phys. Lett.* **1984**, *112*, 94–98.
(61) (a) Dries, T.; Fujara, F.; Kiebel, M.; Rössler, E.; Sillescu, H. *J. Chem. Phys.* **1988**, *88*, 2139–2147. (b) Erratum: Dries, T.; Fujara, F.; Kiebel, M.; Rössler, E.; Sillescu, H. *J. Chem. Phys.* **1989**, *90*, 7613.
(62) Schnauss, W.; Fujara, F.; Sillescu, H. *J. Chem. Phys.* **1992**, *97*, 1378–1389.
(63) Rössler, E.; Eiermann, P. *J. Chem. Phys.* **1994**, *100*, 5237–5248.
(64) Blochowicz, T.; Kudlik, A.; Benkhof, S.; Senker, J.; Rössler, E.; Hinze, G. *J. Chem. Phys.* **1999**, *110*, 12011–12021.
(65) Böhmer, R.; Diezemann, G.; Hinze, G.; Rössler, E. *Prog. NMR Spectrosc.* **2001**, *39*, 191–267.
(66) Vogel, M.; Medick, P.; Rössler, E. A. *Annu. Rep. NMR Spectrosc.* **2005**, *56*, 231–300.
(67) Brodin, A.; Rössler, E. A. *J. Chem. Phys.* **2006**, *125*−1−9.
(68) Brodin, A.; Gainaru, C.; Porokhonskyy, V.; Rössler, E. A. *J. Phys.: Condens. Matter* **2007**, *19*−1−14.
(69) Plazek, D. J. *J. Rheol. (N.Y.)* **1996**, *40*, 987–1014.
(70) Ding, Y.; Sokolov, A. P. *Macromolecules* **2006**, *39*, 3322–3326.
(71) Kimmich, R.; Gille, K.; Fatkullin, N.; Seitter, R.; Hafner, S.; Müller, M. *J. Chem. Phys.* **1997**, *107*, 5973–5978.
(72) Fatkullin, N.; Kimmich, R. *J. Chem. Phys.* **1994**, *101*, 822–832.
(73) Schweizer, K. S. *J. Chem. Phys.* **1989**, *91*, 5802–5821.
(74) Levitz, P.; Korb, J. P.; Petit, D. *Eur. Phys. J. E* **2003**, *12*, 29–33.

MA702771S